



Published in final edited form as:

J Biol Chem. 2004 December 10; 279(50): . doi:10.1074/jbc.M409054200.

Interaction of Calcium-bound C-reactive Protein with Fibronectin Is Controlled by pH:

IN VIVO IMPLICATIONS*

Madathilparambil V. Suresh, Sanjay K. Singh, and Alok Agrawal[‡]

Department of Pharmacology, James H. Quillen College of Medicine, East Tennessee State University, Johnson City, Tennessee 37614

Abstract

C-reactive protein (CRP) binds with high affinity to fibronectin (Fn), a major component of the extracellular matrix (ECM), but at physiological pH the binding is inhibited by calcium ions (Ca^{2+}). Because CRP circulates in the blood in Ca^{2+} -bound form, the occurrence of CRP-Fn interactions *in vivo* has been doubtful. To define the basis of inhibition of CRP-Fn interaction by Ca^{2+} at pH 7.0, we hypothesized that Fn-binding site on CRP consisted of amino acids co-ordinating Ca^{2+} . Site-directed mutagenesis of amino acids co-ordinating Ca^{2+} drastically decreased the binding of CRP to Fn, indicating that the Ca^{2+} -binding site indeed formed the Fn-binding site. To determine the requirements for possible interaction between Ca^{2+} -bound CRP and Fn, we investigated inhibition of CRP-Fn interaction by Ca^{2+} as a function of pH. Ca^{2+} did not inhibit binding of CRP to Fn at pH 6.5 and lower. The contrasting Fn binding properties of CRP at physiological and mildly acidic pH indicated that the interaction of Ca^{2+} -bound CRP with Fn was controlled by pH. We conclude that the inhibition of binding of CRP to Fn by Ca^{2+} at pH 7.0 is a mechanism to prevent CRP-Fn interactions under normal conditions. CRP, in its Ca^{2+} -bound state, is capable of binding Fn but only at the inflammatory sites and tumors with low pH. CRP, Fn, and the ECM all have been implicated in cancer. Taken together our data raise the possibility that CRP-Fn interactions may change the architecture of ECM to modify the development of tumors.

C-reactive protein (CRP)¹ is an evolutionarily conserved plasma protein that is considered to be a multifunctional component of the acute phase response and innate host defense system (1, 2). CRP has been shown to affect the results of the experiments related to diverse pathologic states (3, 4) such as bacterial infection (5, 6), atherosclerosis (7), autoimmune disease (8), and cancer (9). Most proposed functions of CRP depend on its ability to recognize and bind substances of physiologic value (10, 11). By virtue of its wide binding specificities, CRP gets deposited at sites of tissue damage and inflammation (12, 13). Two types of molecular contacts are known for the binding of CRP to its ligands, one that requires calcium ions (Ca^{2+}) and another that does not require Ca^{2+} and instead is inhibited by Ca^{2+} (2). The Ca^{2+} -dependent ligands are primarily the phosphocholine (PCh)-containing substances such as C-polysaccharide (PnC) of the cell wall of *Streptococcus pneumoniae* (10), modified low density lipoprotein (7, 14), and apoptotic cells (14, 15). Ca^{2+} -independent ligands include polycations (16, 17) and the extracellular matrix (ECM) protein

*This work was supported by National Institutes of Health Grant HL071233.

© 2004 by The American Society for Biochemistry and Molecular Biology, Inc.

[‡]To whom correspondence should be addressed: Dept. of Pharmacology, James H. Quillen College of Medicine, East Tennessee State University, P. O. Box 70577, Johnson City, TN 37614. Tel.: 423-439-6336; Fax: 423-439-8773; agrawal@etsu.edu.

¹The abbreviations used are: CRP, C-reactive protein; nCRP, native CRP; Fn, fibronectin; PCh, phosphocholine; PnC, pneumococcal C-polysaccharide; ECM, extracellular matrix; WT, wild type; ELISA, enzyme-linked immunosorbent assay; TBS, Tris-buffered saline; mAb, monoclonal antibody; BSA, bovine serum albumin.

fibronectin (Fn) (18, 19). In this paper we report the mechanism of CRP-Fn interactions and discuss their suitability for *in vivo* circumstances.

CRP is one of the pentraxin proteins composed of 5 identical 206-amino acid-long subunits (20, 21). All five subunits have the same orientation in the pentamer, with a Ca^{2+} -binding site and a PCh-binding site located on the same face of each subunit (2). Each Ca^{2+} site occupies two Ca^{2+} . Using synthetic peptides derived from CRP, direct binding of Ca^{2+} to a peptide of residues 134–148 has been shown (22). Crystallography of $\text{CRP}\cdot\text{Ca}^{2+}\cdot\text{PCh}$ complex (Fig. 1) has demonstrated that two Ca^{2+} in CRP are co-ordinated by Asp-60, Asn-61, and by residues (Glu-138, Gln-139, Asp-140, Glu-147, and Gln-150) in a loop (23–25). This loop in the absence of bound Ca^{2+} moves away from the main body of the CRP molecule, exposing an otherwise hidden site of proteolysis (26). Bound Ca^{2+} ions protect CRP from proteolytic cleavage and are integral structural elements of CRP. It is believed that CRP circulates in the body in its Ca^{2+} -bound form.

Fn is a multifunctional glycoprotein present in the blood in addition to being the major component of the ECM (27). Fn is also highly expressed in several tumors (28–30). Fn plays key roles in cell adhesion and migration processes in various physiological events, such as wound healing, thrombosis, tissue remodeling, and cancer (27, 28). Thus, understanding the nature of CRP-Fn interaction and its impact on each other's functions is of importance.

Some features of CRP-Fn interaction have been reported a decade ago (10, 18, 19). CRP-Fn interaction does not require Ca^{2+} , and the maximal interaction occurs at pH 5.0. At physiological pH it has been shown that Ca^{2+} inhibits binding of CRP to Fn (18). We hypothesized (31) that the Fn-binding site consisted of amino acids in CRP that co-ordinated Ca^{2+} . In the present study our main goal was to define the mechanism of CRP-Fn interactions so as to validate the occurrence of CRP-Fn interactions *in vivo*. Our data indicated that the Ca^{2+} site of CRP participated in binding to Fn and provided an explanation for the inhibitory role of Ca^{2+} on CRP-Fn interaction. Furthermore, at pH 7.0 Ca^{2+} inhibited CRP-Fn interaction, whereas at pH 6.5 and lower it did not. These findings support that *in vivo* Ca^{2+} -bound CRP has the capability of interacting with Fn but exclusively at the ECM of the inflammatory sites including carcinomas where the pH goes down.

EXPERIMENTAL PROCEDURES

Construction and Expression of CRP Mutants

We constructed CRP cDNA encoding E138A, Q139A, D140A, E147A, E147Q, E147K, Q150A, D60A, N61A, and D60A/E147A mutants. The WT human CRP cDNA in the expression vector p91023 (32) was used as the template for construction of cDNA-encoding proteins with single amino acid substitutions. The D60A mutant CRP cDNA was used as a template to construct cDNA for the D60A/E147A CRP. Site-directed mutagenesis was conducted using the QuikChange mutagenesis kit (Stratagene). Mutagenic oligonucleotides (Fig. 2) were designed according to the kit instructions and obtained from Integrated DNA Technologies. Mutations were verified by sequencing performed in our Core Facility. Two clones for each mutant were purified using the maxiprep plasmid isolation kit (Eppendorf). COS cells were used for protein expression and cultured as described previously (31). Cells (2×10^6) were transfected with 5 μg of the plasmids containing mutant CRP cDNA using FuGENE 6 (Roche Applied Science). At 96 h post-transfection, culture media were collected, and the expression of CRP was determined by employing ELISA.

Purification of CRP

The WT native CRP (nCRP) was purified from ascitic fluid, and WT recombinant CRP was purified from the culture medium of the stable Chinese hamster ovary cell line (31) by three steps, a Ca^{2+} -dependent affinity chromatography on a PCh-Sepharose column (Pierce) followed by an anion-exchange chromatography on a Mono Q column and a gel filtration on a Superose12 column (GE Healthcare) using the Biologic Duo Flow Protein Purification System (Bio-Rad). Mutants of CRP were purified from culture media by affinity chromatography alone as before (31). Briefly, culture media were passed through the PCh-Sepharose in a Ca^{2+} -containing buffer, and the bound CRP was eluted with an EDTA-containing buffer. CRP-positive fractions, identified by ELISA, were pooled and dialyzed against TBS (10 mM Tris-HCl, pH 7.2, 150 mM NaCl).

CRP ELISA

The concentration of CRP was estimated using ELISA (31). A polyclonal anti-CRP antibody (1/1000 dilution; Sigma) was used as the capture antibody, and the affinity-purified anti-CRP mAb HD2.4 (0.5 $\mu\text{g}/\text{ml}$) was used as the reporter. The HD2.4 mAb was affinity-purified from the cell culture supernatant of a hybridoma cell line (ATCC). Standard curves were constructed with purified nCRP (3.13–100 ng/ml) diluted in TBS, 0.1% gelatin, 0.01% Tween 20. Horseradish peroxidase-conjugated goat anti-mouse IgG H+L (Pierce) was used as the secondary antibody. Color was developed with 300 $\mu\text{g}/\text{ml}$ ABTS chromophore, diammonium salt (Calbiochem), 0.03% H_2O_2 in 0.5 M citrate buffer, pH 4.0, and measured at 405 nm in the microtiter plate reader (Molecular Devices).

PCh Binding Assay

Binding activity of CRP for PCh-containing ligands was evaluated by two assays using PCh-BSA (Biosearch Technologies) and PnC (Statens Seruminstitut) (31). Briefly, microtiter wells were coated with either PCh-BSA (10 $\mu\text{g}/\text{ml}$) or PnC (2 $\mu\text{g}/\text{ml}$). Culture media were diluted to appropriate concentrations in TBS-Ca (TBS, 0.1% gelatin, 0.01% Tween 20, 5 mM CaCl_2). Purified nCRP (3.13–100 ng/ml) was used to construct standard curves. Bound CRP was detected as in ELISA. In some experiments binding curves were constructed by using serial dilutions of purified WT and mutant CRP, covering the range from 1.56 to 200 ng/ml.

Fn Binding Assay

The binding of CRP to Fn was assessed under 2 conditions unless otherwise mentioned, pH 7.0 and 5.0, using previously published methods (18, 31) with some modifications. For the assay at pH 5.0, CRP was dialyzed against TBS, pH 5.0, and tested for Fn binding activity (in addition to ELISA and PCh binding) within 72 h. Microtiter wells were coated with Fn (Sigma, F2006) at a concentration of 2 $\mu\text{g}/\text{ml}$ in TBS, pH 7.0, overnight at room temperature. Wells were blocked with TBS containing 0.1% BSA. The binding curves were constructed using serial dilutions of purified WT and mutant CRP, covering the concentration range from 0.156 to 10 $\mu\text{g}/\text{ml}$ in either buffer A (TBS, pH 7.0, 0.01% Tween 20) or buffer B (TBS, pH 5.0, 0.01% Tween 20) with and without 5 mM CaCl_2 . After a 3-h incubation at room temperature, the wells were washed with buffer A. Affinity-purified polyclonal rabbit anti-CRP antibody (1 $\mu\text{g}/\text{ml}$) was used as a reporter to detect bound CRP. The reporter antibody was purified from the anti-CRP antibody (Sigma) by affinity chromatography on a CRP-conjugated agarose column prepared by using the AminoLink Immobilization kit (Pierce). Wells were developed with horseradish peroxidase-conjugated goat anti-rabbit IgG H+L (Pierce) as in ELISA.

Polycation Binding Assay

Binding activity of CRP for polycationic ligands was evaluated by two assays using poly-L-arginine (Sigma, P-3892, M_r 70,000–150,000) and poly-L-lysine (Sigma, P8920, M_r 150,000–300,000, 0.01% solution). Microtiter wells were coated with either poly-L-arginine (10 $\mu\text{g}/\text{ml}$) or poly-L-lysine (0.002%) in TBS overnight at 4 °C. After blocking the wells with TBS containing 0.5% gelatin, purified WT and mutant CRP that were serially diluted (1.56–100 ng/ml) in TBS containing 0.1% gelatin and 0.01% Tween 20 were added to the wells and incubated overnight at 4 °C. Bound CRP was detected as in ELISA.

Gel Filtration

Gel filtration analyses of purified WT and mutant CRP dialyzed against pH 5.0 buffer was carried out on a Superose12 column (GE Healthcare) using the Biologic Duo Flow Protein Purification System (Bio-Rad). Affinity-purified CRP preparations (250 μl , ~10 μg depending upon the concentrations of the stocks) were injected into the column and eluted with TBS at a flow rate of 200 $\mu\text{l}/\text{min}$. Sixty fractions (300 μl each) were collected, and CRP-containing fractions were located by ELISA. Purified nCRP at pH 7.0 was used to determine the elution volume for the pentameric CRP.

Ca²⁺-Site Proteolytic Cleavage Assay

The Ca²⁺-binding site-dependent proteolytic cleavage assay of CRP was conducted as described previously (26) with modifications. WT and mutant CRP (4 μg) in TBS (pH 7.0 or 5.0) were incubated with 1 μg of protease (from *Streptococcus griseus*, Sigma, P6911) with and without 5 mM CaCl₂ for 2 h at 37 °C. Digestion mix was then incubated with 20 μl of packed volume of anti-CRP-Sepharose beads for 1 h at 37 °C to separate CRP from the enzyme. The conjugation of affinity-purified polyclonal anti-CRP antibody to Sepharose was performed using the AminoLink Immobilization kit (Pierce). The beads were then washed with TBS, re-suspended in TBS, and subjected to SDS-PAGE on a 4–20% polyacrylamide gradient gel under reducing conditions. The gels were stained with silver stain (Bio-Rad). The Bio-Rad broad-range marker was used as the molecular weight standard.

RESULTS

Construction, Expression, and Purification of Mutant CRP

Ten CRP cDNAs encoding E138A, Q139A, D140A, E147A, E147Q, E147K, Q150A, D60A, N61A, and the double mutant D60A/E147A were constructed. Expression was determined by ELISA performed on the culture supernatants of transfected COS cells. Despite repeated transfections using duplicate clones, under a wide variety of experimental conditions the CRP mutants Q139A, D140A, and N61A were not expressed at all and could not be pursued further. Expression levels of CRP mutants E138A and Q150A were low (range, 5–100 ng/ml), enough to test their PCh binding activity but not enough to test their Fn binding activity. The other five CRP mutants involving Glu-147 and Asp-60 were successfully expressed, and their expression levels (1000–3000 ng/ml) were similar to that of the WT recombinant CRP.

To determine the effect of mutating the Ca²⁺-site on the binding of CRP to PCh and to design a purification strategy for the expressed proteins, PCh binding assays using PnC and PCh-BSA were performed on culture media containing WT and mutant CRP. Data from the PnC assays are presented (Fig. 3); PCh-BSA gave similar results. Values shown reflect the avidity of individual CRP species for PCh relative to nCRP, whose PCh binding activity was taken as unity. WT and the five CRP mutants that were equally expressed bound to PCh efficiently. Because binding of CRP to PCh requires binding of Ca²⁺ to CRP first, these data

indicated that the mutation of a single amino acid, Glu-147 or Asp-60, did not affect the binding of CRP to Ca^{2+} . The binding of E138A CRP to PCh was reduced by more than half compared with WT CRP. The Q150A CRP failed to bind to PCh. The mutants E138A and Q150A were not analyzed further. CRP mutants with substituted Glu-147 and Asp-60 could be purified by PCh chromatography for further characterization.

Binding of CRP to Fn

As shown in Fig. 4A, nCRP bound to Fn at pH 7.0 in a dose-dependent manner. In the presence of 5 mM CaCl_2 , the binding was inhibited throughout the CRP dose-response. At pH 7.0, inhibition of the binding of CRP (10 $\mu\text{g}/\text{ml}$) to Fn was dependent on the concentration of Ca^{2+} (Fig. 4B), with maximum inhibition at ~ 2 mM CaCl_2 . Although 2 mM CaCl_2 was sufficient to inhibit binding of CRP to Fn, 5 mM CaCl_2 was chosen for subsequent experiments to ensure that Ca^{2+} was in excess. The binding of various purified CRP mutants to Fn at pH 7.0 was evaluated next (Fig. 4C). Mutations of Asp-60 to Ala and of Glu-147 to Ala/Gln resulted in a 70–95% decrease in the binding of CRP to Fn compared with that of WT CRP. The decrease was most pronounced when Glu-147 was substituted with Lys or when both residues were mutated to Ala.

Because maximal binding of CRP to Fn occurs at pH 5.0 (18), we tested the binding of CRP mutants to Fn at pH 5.0 (Fig. 4D). Again, the binding of CRP mutants E147K and D60A/E147A to Fn was reduced by 80–90 and 50–60% respectively, and this decrease was observed throughout the dose-response. Unlike at pH 7.0, D60A, E147A, and E147Q CRP mutants efficiently bound to Fn at pH 5.0. We, therefore, determined the effects of Ca^{2+} on the binding of these CRP mutants to Fn at pH 5.0 (Fig. 4E). For clarity, the results are shown only for the WT CRP and two mutants, E147A and D60A. To our surprise Ca^{2+} did not inhibit the binding of mutant CRP to Fn at pH 5.0 and did not even inhibit the binding of nCRP to Fn at pH 5.0. Binding of other mutants to Fn at pH 5.0 was also not inhibited by Ca^{2+} (data not shown). These results clearly indicate that the inhibition of CRP-Fn interaction by Ca^{2+} occurs only at pH 7.0 and not at pH 5.0. Next, we determined the inhibition of the binding of CRP to Fn by Ca^{2+} at pH values varying from 4.0 to 7.0 (Fig. 4F). The binding of CRP to Fn was inhibited about 70% at pH 7.0, as before. Unexpectedly, the binding was inhibited by only 10% at pH 6.5, and no inhibition was observed at pH 6.0 and lower.

Assessment of the Overall Structure of CRP

We investigated the possibility that dialysis of CRP against TBS, pH 5.0, might have perturbed the overall structure of CRP. Although the ELISA performed on CRP at pH 5.0 indicated that CRP retained its reactivity toward the mAb, 3 more assays were utilized; PnC binding assay (Fig. 5A), gel filtration (Fig. 5B), and Ca^{2+} -site-dependent proteolytic cleavage assay (Fig. 5C). WT and all mutant CRP bound to PnC in a dose-dependent manner and produced essentially overlapping curves, indicating that their PCh binding activities were retained at pH 5.0. Gel filtration to assess pentameric nature of the dialyzed mutant CRP showed that the elution volume of all CRP mutants at pH 5.0 was similar to that of nCRP at pH 7.0. Data are shown only for 3 mutants at pH 5.0; elution profiles of nCRP and other mutants at pH 5.0 were identical. Last, at both pH 7.0 and 5.0, in the absence of Ca^{2+} , nCRP was cleaved by the protease, generating 3 fragments as reported previously (26), and at both pH values, Ca^{2+} protected CRP from proteolytic cleavage. Combined results indicated that the overall structure of CRP was not altered at pH 5.0.

Binding of CRP to Polycations

To evaluate whether the Ca^{2+} site binds only Fn or it binds, in general, to all Ca^{2+} -independent ligands of CRP, an assay was set up to determine binding of CRP to

polycations. We expected that the Fn site and the polycation site on CRP would be the same since Ca^{2+} was also found to inhibit CRP-polycation interaction (34). Substitution of Glu-147 with Lys and the double mutation of Asp-60/Glu-147 to Ala abolished the binding of CRP to poly-L-arginine (Fig. 6A). Although D60A CRP bound polycations and the binding of E147A and E147Q to the two polycations was different (Fig. 6B), the results indicated that the Ca^{2+} site did participate in the binding of CRP to its Ca^{2+} -independent ligands including Fn and polycations.

Effect of Ca^{2+} Site Mutations on the Proteolytic Cleavage of CRP

As a result of mutating Asp-60 and Glu-147, we discovered a loss of Fn binding activity and polycation binding activity but not of PCh binding (and, thus, not of Ca^{2+} binding) activity. This indicated that the structure of the Ca^{2+} site of Ca^{2+} -bound nCRP was different from that of Ca^{2+} -bound mutant CRP. To support this conclusion, we examined the topology of Ca^{2+} site by protease cleavage assay (Fig. 7). Protease treatment of nCRP in the absence of Ca^{2+} generated three fragments (*lane 3*). The fragments designated A1 and A2 were found to be of 17 and 16 kDa, and fragment B was estimated to be of 6 kDa, consistent with the previous reports (26). nCRP was completely protected from digestion in the presence of Ca^{2+} (*lane 4*). The E147A CRP was cleaved in the absence of Ca^{2+} , generating only two fragments (*lane 6*), and in the presence of Ca^{2+} , cleavage was not protected; instead all three fragments were produced (*lane 7*). The D60A CRP was not susceptible to protease at all (*lanes 9 and 10*). The effect of mutating Asp-60 was not apparent in the cleavage of the double mutant (*lanes 12 and 13*). These data confirmed that the configuration of the Ca^{2+} site of Ca^{2+} -bound mutants was different from that of Ca^{2+} -bound nCRP.

DISCUSSION

CRP circulates in the body in its Ca^{2+} -bound form, and Ca^{2+} inhibits binding of CRP to Fn. Therefore, the occurrence of CRP-Fn interactions *in vivo* has been uncertain. We investigated the Fn-binding site on CRP and the mechanism of binding of CRP to Fn to determine the conditions for possible interaction between Ca^{2+} -bound CRP and Fn. Our major findings were as follows. 1) Ca^{2+} inhibited binding of CRP to Fn at pH 7.0 but not at pH 6.5 and lower. No inhibition was seen at pH 5.0, the pH demonstrated for the maximal binding of CRP to Fn. 2) The Ca^{2+} site of CRP participated in binding to Fn, and the same site was found to be the polycation-binding site. 3) Mutations of Asp-60 or Glu-147 at the Ca^{2+} site of CRP abolished Fn binding at pH 7.0 but not at pH 5.0. 4) Mutations of Asp-60 or Glu-147 did not abolish PCh binding and Ca^{2+} binding. 5) Substitution of Asp-60 with Ala conferred resistance to CRP against proteolytic cleavage. 6) CRP, at a pH as low as 5.0, retained its pentameric form, ability to bind Ca^{2+} and PCh, reactivity with a mAb, and susceptibility toward the protease.

Based on the expression levels of CRP mutants, 7 amino acids forming the Ca^{2+} site can be divided into two groups; group 1 with Asp-60 and Glu-147 and group 2 with Asn-61, Glu-138, Gln-139, Asp-140, and Gln-150. CRP mutants of group 1 residues were expressed and bound PCh, reflecting their binding to Ca^{2+} also. CRP mutants of group 2 residues were either not expressed or poorly expressed with the loss of Ca^{2+} binding and PCh binding ability. These results indicated that the group 2 residues were critical for binding to Ca^{2+} and for maintaining the native structure of CRP. Expression pattern of various CRP mutants favor the notion that binding of Ca^{2+} to CRP occurs during its biosynthesis and is a prerequisite for the correct folding and assembly of the protein, and perhaps this may be a general phenomenon for other Ca^{2+} -binding proteins.

The inability of group 2 CRP mutants to be expressed was not surprising in view of the crystallographic data on Ca^{2+} -bound CRP (23–25). Each CRP subunit binds 2 Ca^{2+} , Ca^{2+} -1

and Ca^{2+} -2. Ca^{2+} -1 is co-ordinated by Asp-60, Asn-61, Glu-138, Gln-139, and Asp-140. Asp-60 provides only one oxygen ligand to Ca^{2+} -1. Ca^{2+} -2 is co-ordinated by Glu-138, Asp-140, Glu-147, and Gln-150. In the crystal packing, CRP was still bound to one Ca^{2+} when Glu-147 was not co-ordinated to Ca^{2+} -2 but was co-ordinated to Phe-66 from the neighboring pentamer. Thus, Asn-61, Glu-138, Gln-139, Asp-140, and Gln-150 are involved more than Asp-60 and Glu-147 in co-ordinating Ca^{2+} .

Analyses of group 1 CRP mutants, D60A and E147A, were sufficient to provide data to support the hypothesis that the Ca^{2+} site of CRP participated in binding not only to Fn but also to polycations (31, 35). The loss of Fn binding activity of these CRP mutants at pH 7.0 suggested that the amino acids in CRP that coordinated Ca^{2+} were also required for binding to Fn. On the other hand, it was unlikely that these 2 amino acids were the contact residues because their mutations did not abolish binding of CRP to Fn at pH 5.0. Loss of binding of CRP to Fn at pH 7.0 due to these mutations could be due to a change in the disposition of the Ca^{2+} binding loop in the mutant CRP. This conclusion is supported by the data showing altered susceptibility of these mutants to proteolytic cleavage.

The definition of the Fn-binding site of CRP can be derived from the observed effects of acidic pH on CRP-Fn interaction. Although we did not find a difference in the Ca^{2+} site of CRP at pH 7.0 *versus* 5.0 using PCh binding and proteolytic cleavage assays, a pH 6.3-dependent conformational change in CRP has been shown previously by circular dichroism and fluorescence spectra analyses (36). Assuming that the pH lower than 6.0 results in the loss of binding of one Ca^{2+} per CRP subunit, creating half of the Ca^{2+} site vacant, and that Fn utilizes that portion of the Ca^{2+} site to bind, then CRP can bind to PCh and to Fn despite mutations of Asp-60 and Glu-147. It is not known whether two Ca^{2+} per CRP subunit is an absolute necessity for CRP-PCh interaction. The finding that the CRP-Fn interaction is inhibited in a dose-dependent manner by relatively higher concentrations of Ca^{2+} at pH 7.0 also supports that the vacancy of entire Ca^{2+} site is not required for binding to Fn. The Fn-binding site may also include the hydrophobic pocket located adjacent to the PCh-binding site of CRP (23–25). We hypothesize that the Fn-binding site of CRP is composed of the Ca^{2+} site occupied with only one Ca^{2+} , and formation of such a site is the consequence of low pH-induced conformational change in and around the Ca^{2+} site. A similar proposal involving a conformational change has been proposed for the binding of Fn to vascular endothelial growth factor whose binding to Fn also increases at acidic pH (37).

We propose that the inhibition of binding of CRP to Fn by Ca^{2+} at physiological pH serves as a mechanism to prevent CRP-Fn interaction in the ECM of normal tissues. The Ca^{2+} -bound CRP gains the capacity to interact with Fn, exclusively at the ECM of the inflammatory sites. One characteristic feature of the inflammatory sites, also of the tumors, is local acidosis, resulting in a pH that can be as low as 5.8 (36, 38). The architecture of the ECM in tumors is different from normal tissues. Possible CRP-Fn interaction at the ECM of tumor sites is relevant because both Fn (28) and CRP (39–41) are present at tumor sites. Recently, a polymeric form of Fn has been shown to have antitumor properties (42). The ability of CRP to convert Fn into polymeric Fn is not known, but CRP may modify the ECM around the tumors to look it more like ECM of normal tissues. CRP, monomeric CRP and the CRP-derived peptides, all have been shown to inhibit tumor metastases in experimental models of cancer (9, 43, 44). Involvement of Fn in these *in vivo* antitumor actions of CRP is yet to be discovered, but while investigating the regulation of CRP-Fn interaction by pH, we made an unexpected observation that the denatured CRP bound Fn more avidly than pentameric CRP did.² These findings strongly raise the possibility that CRP-Fn interaction might play a role in modulating the progression of cancer.

²M. V. Suresh and A. Agrawal, unpublished data.

All studies on CRP-Fn interaction so far have utilized plasma Fn representing ECM Fn. However, under inflammatory conditions there are many alternatively spliced forms of Fn expressed at various other sites *in vivo* (45). For example, in atherosclerotic lesions, alternatively spliced Fn have been found (46) in addition to the deposition of CRP at such lesions (3, 4). Alternatively spliced forms of Fn are also expressed on activated T lymphocytes (47), and interestingly, CRP binds to activated T lymphocytes (48). We do not know if the mechanisms we report here for the interaction between CRP and plasma Fn would be the same for the interaction between CRP and alternatively spliced forms of Fn. It is a possibility that Ca²⁺-bound CRP might interact with alternatively spliced forms of Fn even at physiological pH. Existence of low pH at tumor ECM and expression of Fn at sites other than ECM such as atherosclerotic lesions and the T lymphocytes provide opportunity to investigate the functions of CRP-Fn complexes.

In summary, the interaction of circulating Ca²⁺-bound CRP with Fn is controlled by pH. In normal physiological conditions, binding of Ca²⁺ to CRP prevents interaction with Fn at the ECM. At the ECM of the inflammatory sites with low pH, such as in tumors, Ca²⁺-bound CRP gains the capability to interact with Fn. Because CRP, Fn, and the ECM all have been implicated in cancer, we propose that CRP-Fn interactions may change the architecture of ECM to modify the course of the disease progression.

References

1. Kushner I. *Ann N Y Acad Sci.* 1982; 382:39–48. [PubMed: 6952807]
2. Volanakis JE. *Mol Immunol.* 2001; 38:189–197. [PubMed: 11532280]
3. Hirschfield GM, Pepys MB. *QJM.* 2003; 96:793–807. [PubMed: 14566035]
4. Jialal I, Devaraj S, Venugopal SK. *Hypertension.* 2004; 44:6–11. [PubMed: 15148294]
5. Mold C, Rodic-Polic B, Du Clos TW. *J Immunol.* 2002; 168:6375–6381. [PubMed: 12055255]
6. Yother J, Volanakis JE, Briles DE. *J Immunol.* 1982; 128:2374–2376. [PubMed: 7061864]
7. Bhakdi S, Torzewski M, Paprotka K, Schmitt S, Barsoom H, Suriyaphol P, Han SR, Lackner KJ, Husmann M. *Circulation.* 2004; 109:1870–1876. [PubMed: 15037531]
8. Szalai AJ, Weaver CT, McCrory MA, van Ginkel FW, Reiman RM, Kearney JF, Marion TN, Volanakis JE. *Arthritis Rheum.* 2003; 48:1602–1611. [PubMed: 12794828]
9. Deodhar SD, James K, Chiang T, Edinger M, Barna BP. *Cancer Res.* 1982; 42:5084–5088. [PubMed: 7139613]
10. Agrawal A, Xu Y, Ansardi D, Macon KJ, Volanakis JE. *J Biol Chem.* 1992; 267:25352–25358.
11. Hack CE, Wolbink GJ, Schalkwijk C, Speijer H, Hermens WT, van den Bosch H. *Immunol Today.* 1997; 18:111–115. [PubMed: 9078682]
12. Du Clos TW, Mold C, Paterson PY, Alroy J, Gewurz H. *Clin Exp Immunol.* 1981; 43:565–573. [PubMed: 7026095]
13. Kushner I, Kaplan MH. *J Exp Med.* 1961; 114:961–973. [PubMed: 14460901]
14. Chang MK, Binder CJ, Torzewski M, Witztum JL. *Proc Natl Acad Sci U S A.* 2002; 99:13043–13048. [PubMed: 12244213]
15. Gershov D, Kim S, Brot N, Elkon KB. *J Exp Med.* 2000; 192:1353–1363. [PubMed: 11067883]
16. Di Camelli R, Potempa LA, Siegel J, Suyehira L, Petras K, Gewurz H. *J Immunol.* 1980; 125:1933–1938. [PubMed: 6776184]
17. Lee RT, Takahara I, Lee YC. *J Biol Chem.* 2002; 277:225–232. [PubMed: 11684681]
18. Salonen EM, Vartio T, Hedman K, Vaheri A. *J Biol Chem.* 1984; 259:1496–1501. [PubMed: 6693419]
19. Tseng J, Mortensen RF. *Mol Immunol.* 1988; 25:679–686. [PubMed: 2460754]
20. Osmand AP, Friedenson B, Gewurz H, Painter HP, Hofmann T, Shelton E. *Proc Natl Acad Sci U S A.* 1977; 74:739–743. [PubMed: 265538]
21. Gotschlich EC, Edelman GM. *Proc Natl Acad Sci U S A.* 1965; 54:558–566. [PubMed: 5217443]

22. Mullenix MC, Mortensen RF. *Mol Immunol.* 1994; 8:615–622. [PubMed: 8196672]
23. Shrive AK, Cheetham GMT, Holden D, Myles DAA, Turnell WG, Volanakis JE, Pepys MB, Bloomer AC, Greenhough TJ. *Nat Struct Biol.* 1996; 3:346–354. [PubMed: 8599761]
24. Thompson D, Pepys MB, Wood SP. *Structure Fold Des.* 1999; 7:169–177. [PubMed: 10368284]
25. Ramadan MAM, Shrive AK, Holden D, Myles DAA, Volanakis JE, DeLucas LJ, Greenhough TJ. *Acta Crystallogr Sect D.* 2002; 58:992–1001. [PubMed: 12037301]
26. Kinoshita CM, Ying SC, Hugli TE, Siegel JN, Potempa LA, Jiang H, Houghten RA, Gewurz H. *Biochemistry.* 1989; 28:9840–9848. [PubMed: 2692716]
27. Magnusson MK, Mosher DF. *Arterioscler Thromb Vasc Biol.* 1998; 18:1363–1370. [PubMed: 9743223]
28. Ruoslahti E. *Adv Cancer Res.* 1999; 76:1–20. [PubMed: 10218097]
29. David L, Nesland JM, Holm R, Sobrinho-Simoes M. *Cancer.* 1994; 73:518–527. [PubMed: 8299074]
30. Ioachim E, Charchanti A, Briasoulis E, Karavasilis V, Tsanou H, Arvanitis DL, Agnantis NJ, Pavlidis N. *Eur J Cancer.* 2002; 38:2362–2370. [PubMed: 12460779]
31. Agrawal A, Simpson MJ, Black S, Carey MP, Samols D. *J Immunol.* 2002; 169:3217–3222. [PubMed: 12218140]
32. Agrawal A, Lee S, Carson M, Narayana SVL, Greenhough TJ, Volanakis JE. *J Immunol.* 1997; 158:345–350. [PubMed: 8977209]
33. Woo P, Korenberg JR, Whitehead AS. *J Biol Chem.* 1985; 260:13384–13388. [PubMed: 3840479]
34. Potempa LA, Siegel JN, Gewurz H. *J Immunol.* 1981; 127:1509–1514. [PubMed: 7276568]
35. Black S, Agrawal A, Samols D. *Mol Immunol.* 2003; 39:1045–1054. [PubMed: 12749911]
36. Miyazawa K, Inoue K. *J Immunol.* 1990; 145:650–654. [PubMed: 2365997]
37. Goerges AL, Nugent MA. *J Biol Chem.* 2004; 279:2307–2315. [PubMed: 14570917]
38. Wike-Hooley JL, Haveman J, Reinhold HS. *Radiother Oncol.* 1984; 2:343–366. [PubMed: 6097949]
39. Berman MA, Burnham JA, Sheahan DG. *Hum Pathol.* 1988; 19:784–794. [PubMed: 2456977]
40. Hurlimann J, Gardiol D. *Am J Surg Pathol.* 1991; 15:280–288. [PubMed: 1847609]
41. Nozoe T, Korenaga D, Futatsugi M, Saeki H, Maehara Y, Sugimachi K. *Cancer Lett.* 2003; 192:89–95. [PubMed: 12637157]
42. Yi M, Ruoslahti E. *Proc Natl Acad Sci U S A.* 2001; 98:620–624. [PubMed: 11209058]
43. Kresl JJ, Potempa LA, Anderson B, Radosevich JA. *Tumour Biol.* 1999; 20:72–87. [PubMed: 10050106]
44. Barna BP, Eppstein DA, Thomassen MJ, Nestor JJ Jr, Ho T, Medendorp SV, Deodhar SD. *Cancer Immunol Immunother.* 1993; 36:171–176. [PubMed: 8439977]
45. Pankov R, Yamada KM. *J Cell Sci.* 2002; 115:3881–3883.
46. Tan MH, Sun Z, Opitz SL, Schmidt TE, Peters JH, George EL. *Blood.* 2004; 104:11–18. [PubMed: 14976060]
47. Wagner C, Pioch M, Meyer C, Iking-Konert C, Andrassy K, Hänsch GM. *J Mol Med.* 2000; 78:337–345. [PubMed: 11001531]
48. Mortensen RF, Osmand AP, Gewurz H. *J Exp Med.* 1975; 141:821–839. [PubMed: 1092791]

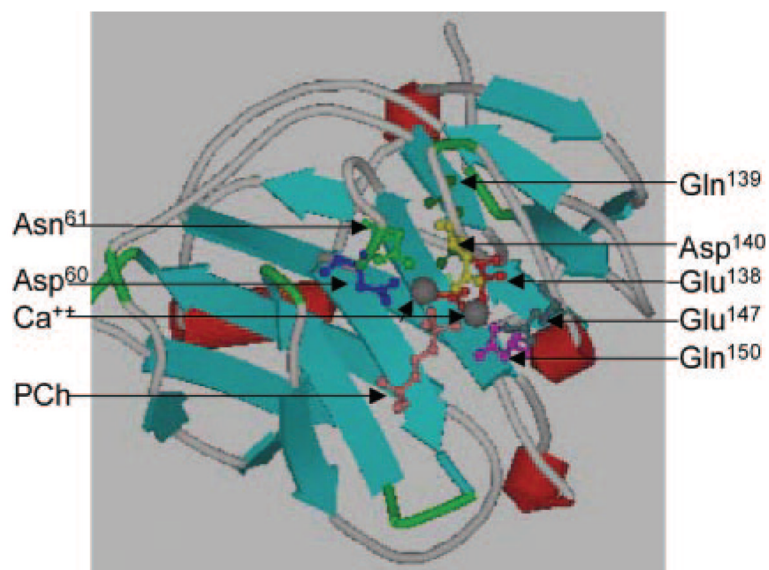


Fig. 1. Ca^{2+} -binding site of CRP

The ViewerPro 4.2 software (Accelrys Inc.) was used to generate ribbon diagram of the crystal structure of CRP- Ca^{2+} · PCh complex (24) obtained from Brookhaven Protein Data Bank. A portion of one of the five subunits is shown. The side chains of seven amino acids co-ordinating two Ca^{2+} are *highlighted*. Ca^{2+} ions are in *gray*, and the PCh molecule is in *orange*.

Mutant	Mutagenic oligo
D60A	5'-CCACCAAGAGACAAG CC AATGAGATTCTCA 3'-GGTGGTTCTCTGTT CG TTACTCTAAGAGT
N61A	5'-GCCACCAAGAGACAAGAC GC TGAGATTCTCATATT 3'-CGGTGGTTCTCTGTTCTG CGA CTCTAAGAGTATAA
E138A	5'-CATCATCTTGGGGCAGG CG CAGGATTCCCTTCG 3'-GTAGTAGAACCCCGTCC GC CTCCTAAGGAAGC
Q139A	5'-CATCTTGGGGCAGGAG GC CGATTCCCTTCGGTG 3'-GTAGAACCCCGTCC CGC CTAAGGAAGCCAC
D140A	5'-CTTGGGGCAGGAGCAG CT TCCTTCGGTGGG 3'-GAACCCCGTCTCTCGTCC GA AGGAAGCCACCC
E147A	5'-CGGTGGGAACCTTT CC AGGAAGCCAGTCCCTAG 3'-GCCACCCTTGAAAC GT TCCTTCGGTCAGGGATC
E147Q	5'-CGGTGGGAACCTTT CA AGGAAGCCAGTCCCTAG 3'-GCCACCCTTGAAAG TT TCCTTCGGTCAGGGATC
E147K	5'-CGGTGGGAACCTTT AA AGGAAGCCAGTCCCTAG 3'-GCCACCCTTGAAAT TT TCCTTCGGTCAGGGATC
Q150A	5'-CTTTGAAGGAAGC GC TCCCTAGTGGGAGAC 3'-GAAACTTCCTTCG CG CAGGGATCACCCCTCTG

Fig. 2. Pairs of mutagenic oligonucleotides used in constructing CRP mutants
The sequences were designed based on the published sequence for WT CRP (33). Triplet codons of the mutated amino acids are *boxed*. Mutated bases are in *bold*.

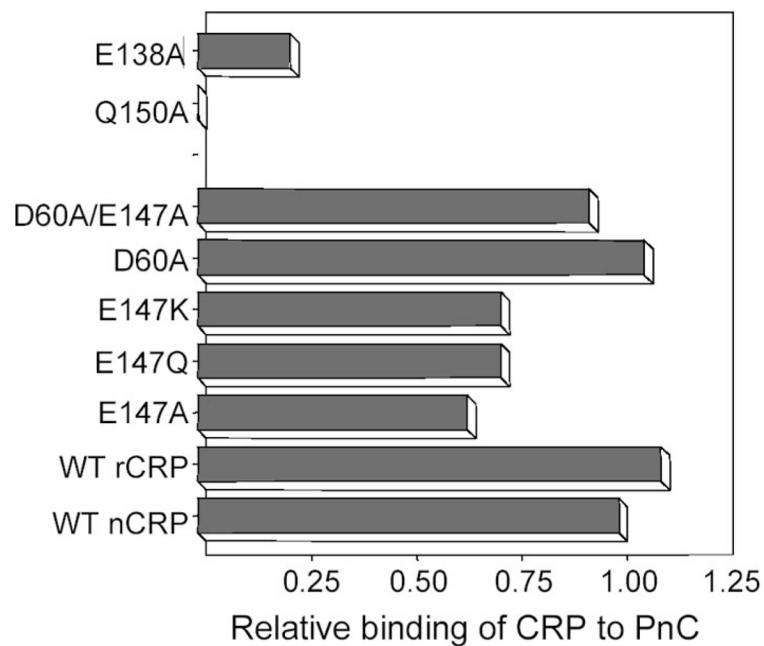


Fig. 3. Binding of CRP to PnC

Microtiter wells were coated with PnC. Culture media containing various CRP species were diluted to ~50 ng/ml in TBS-Ca buffer and added to the wells. Bound CRP was detected using the anti-CRP mAb HD2.4 as reporter. Values on the *x* axis represent the ratio of the concentration of CRP measured by the PnC binding assay over that measured by ELISA run in parallel using nCRP to generate standard curves in both assays.

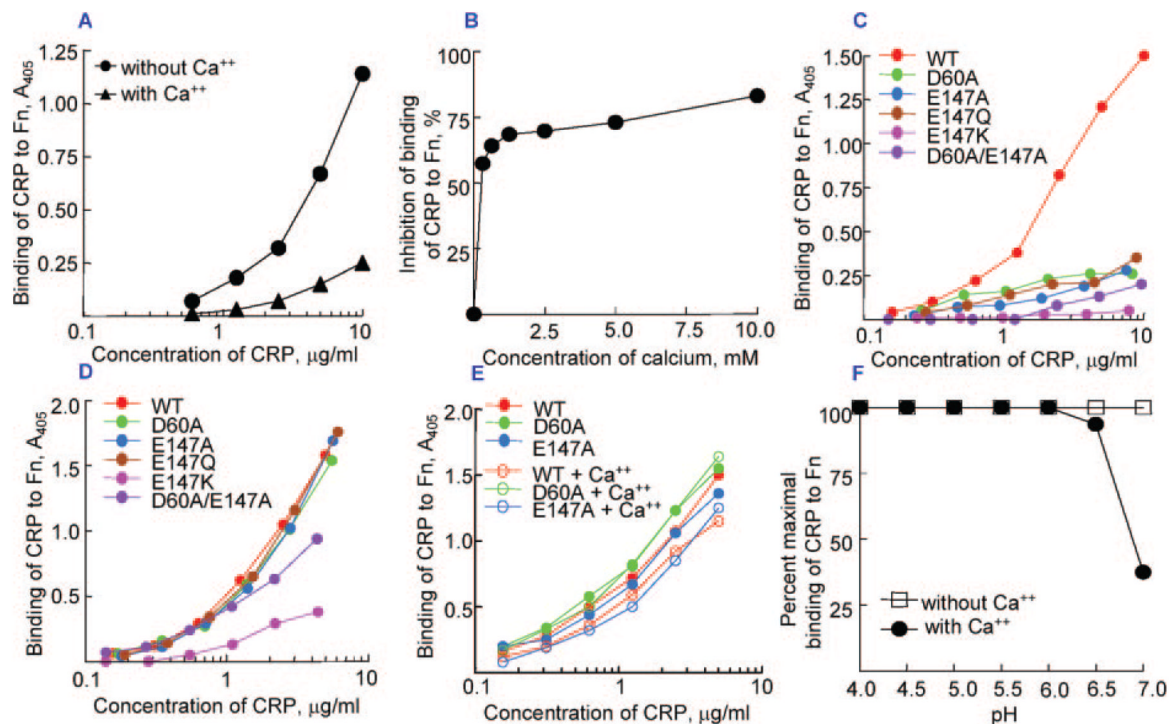


Fig. 4. Binding of CRP to Fn

Microtiter wells were coated with Fn. *A*, increasing concentrations of purified nCRP in TBS, pH 7.0, with and without 5 mM CaCl_2 were added to the wells. *B*, nCRP, 10 $\mu\text{g/ml}$ in TBS, pH 7.0, containing increasing concentrations of CaCl_2 were added to the wells. Binding of CRP to Fn in the absence of CaCl_2 was taken as 100% to calculate percent inhibition. *C*, increasing concentrations of purified WT and mutant CRP in TBS, pH 7.0, without CaCl_2 were added to the wells. *D*, increasing concentrations of purified WT and mutant CRP in TBS, pH 5.0, without CaCl_2 were added to the wells. *E*, increasing concentrations of purified WT and mutant CRP in TBS, pH 5.0, with and without CaCl_2 were added to the wells. *F*, increasing concentrations of purified nCRP, 10 $\mu\text{g/ml}$ in TBS at increasing pH, with and without Ca^{2+} were added to the wells. The binding of CRP to Fn in the absence of Ca^{2+} at various pH was plotted as 100%. In all, bound CRP was detected by using polyclonal anti-CRP antibody as the reporter. All experiments were performed at least three times, and a representative experiment is shown.

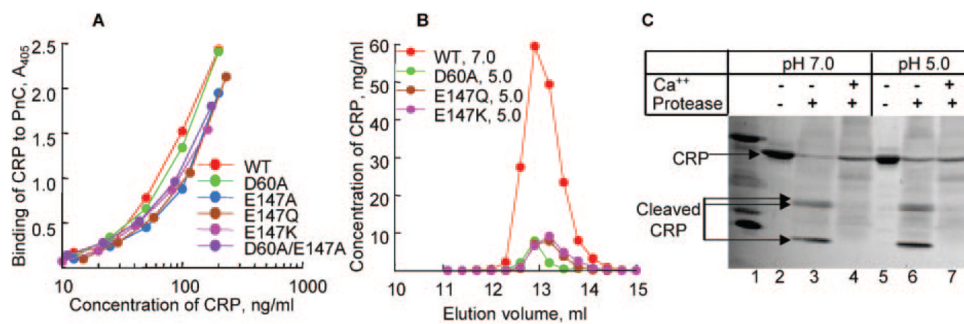


Fig. 5. Effect of pH 5.0 on the overall structure of CRP

A, binding of purified WT and mutant CRP, dialyzed against TBS, pH 5.0, to PnC. Microtiter wells were coated with PnC. Increasing concentrations of various CRP species in a TBS-Ca were added to the wells. Bound CRP was detected by HD2.4 mAb. A representative of two experiments is shown. **B**, elution profiles of purified nCRP at pH 7.0 and purified mutant CRP dialyzed against TBS, pH 5.0, from the Superose12 gel filtration column. **C**, Ca²⁺ site-dependent proteolytic cleavage of CRP. Purified nCRP at pH 7.0 and 5.0 was subjected to proteolytic cleavage in the absence and presence of Ca²⁺. A representative of 2–3 experiments is shown.

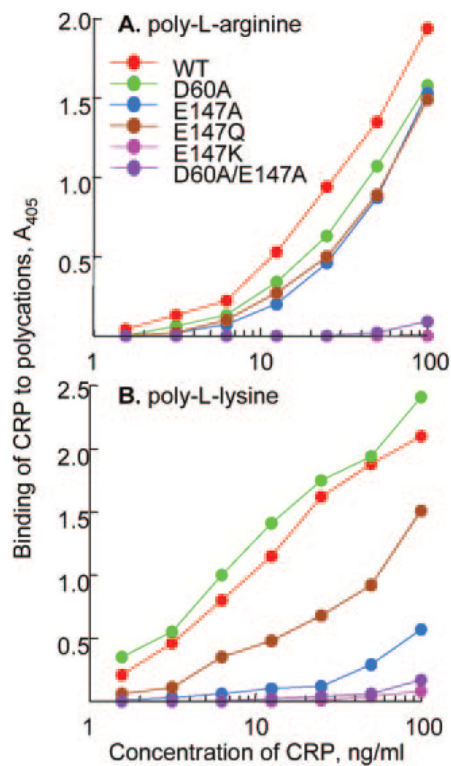


Fig. 6. Binding of CRP to polycations

Microtiter wells were coated with either poly-L-arginine (*A*) or poly-L-lysine (*B*). Increasing concentrations of purified WT and mutant CRP were added to the wells. Bound CRP was detected by HD2.4 mAb. A representative of two experiments is shown.

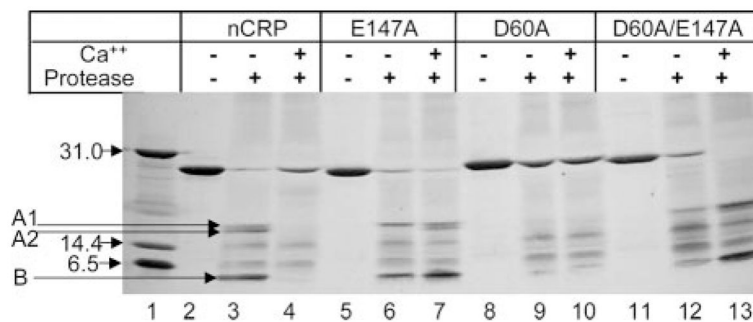


Fig. 7. Ca²⁺ site-dependent proteolytic cleavage of CRP

Reducing SDS-PAGE of WT and mutant CRP treated with protease in the absence and presence of Ca²⁺ was run on a 4–20% polyacrylamide gradient gel. Bands were visualized by silver staining. Before electrophoresis, all CRP samples were incubated with anti-CRP-conjugated agarose beads to remove the protease from CRP. Molecular weight markers are shown in *lane 1*.